APPLIED AND ENVIRONMENTAL MICROBIOLOGY, Oct. 2004, p. 6123–6130 Vol. 70, No. 10
0099-2240/04/$08.00+0 DOI: 10.1128/AEM.70.10.6123–6130.2004

Helix 4 Mutants of the *Bacillus thuringiensis* Insecticidal Toxin Cry1Aa Display Altered Pore-Forming Abilities

Vincent Vachon,[1,2]* Gabrielle Préfontaine,[2,3] Cécile Rang,[4] Florence Coux,[1,2,4] Marc Juteau,[1,2] Jean-Louis Schwartz,[1,2,3] Roland Brousseau,[2,3] Roger Frutos,[4] Raynald Laprade,[1,2] and Luke Masson[2,3]

Groupe d'étude des protéines membranaires, Université de Montréal,[1] and Biocontrol Network[2] and Biotechnology Research Institute,[3] National Research Council, Montreal, Quebec, Canada, and CIRAD, Montpellier, France[4]

Received 23 October 2003/Accepted 15 June 2004

The role played by α-helix 4 of the *Bacillus thuringiensis* toxin Cry1Aa in pore formation was investigated by individually replacing each of its charged residues with either a neutral or an oppositely charged amino acid by using site-directed mutagenesis. The majority of the resulting mutant proteins were considerably less toxic to *Manduca sexta* larvae than Cry1Aa. Most mutants also had a considerably reduced ability to form pores in midgut brush border membrane vesicles isolated from this insect, with the notable exception of those with alterations at amino acid position 127 (R127N and R127E), located near the N-terminal end of the helix. Introducing a negatively charged amino acid near the C-terminal end of the helix (T142D and T143D), a region normally devoid of charged residues, completely abolished pore formation. For each mutant that retained detectable pore-forming activity, reduced membrane permeability to KCl was accompanied by an approximately equivalent reduction in permeability to *N*-methyl-D-glucamine hydrochloride, potassium gluconate, sucrose, and raffinose and by a reduced rate of pore formation. These results indicate that the main effect of the mutations was to decrease the toxin's ability to form pores. They provide further evidence that α-helix 4 plays a crucial role in the mechanism of pore formation.

Bacillus thuringiensis is the most extensively used commercial biopesticide worldwide and is presently the sole source of toxin genes for the development of insect-resistant transgenic plants (13, 15, 42). The insecticidal activity of *B. thuringiensis* is primarily associated with its ability to synthesize a crystalline parasporal inclusion body containing highly specific insecticidal proteins (22, 36). The mode of action of these insecticides involves solubilization of the crystal in the highly alkaline lepidopteran midgut lumen, activation of the toxins by intestinal proteases, recognition of one or more binding sites on the midgut brush border membrane surface followed by pore formation, and cell lysis leading ultimately to insect death (36).

The elucidation by X-ray diffraction analysis of the three-dimensional structures of the activated Cry1Aa (21), Cry2Aa (31), Cry3Aa (28), and Cry3Bb (16) toxins has revealed a common three-domain folding pattern. Domain I is made of seven α-helices, and domains II and III are composed mostly of β-sheets. While domain I is considered to be responsible for pore formation (37, 43, 44), domains II and III are involved in receptor binding and host specificity (11, 12, 24, 47). Domain III is also thought to play a role in protein stability (28). The domains of the activated toxins were shown to interact with each other to yield their overall toxic effect (33, 34). Exchanging domain I from different toxins can affect crystal formation, stability, pore formation, and membrane permeability as well as the size of the pores and toxicity.

* Corresponding author. Mailing address: Groupe d'étude des protéines membranaires, Université de Montréal, P.O. Box 6128, Centre Ville Station, Montreal, Quebec, Canada H3C 3J7. Phone: (514) 343-6111, ext. 3771. Fax: (514) 343-7146. E-mail: vincent.vachon@umontreal.ca.

The toxin is thought to form pores in the cell membrane by first inserting a hairpin composed of the hydrophobic α5 and the amphipathic α4 helices (3, 30, 37). In agreement with this mechanism, mutation analyses conducted on the various helices of domain I have shown that, except for a few specific residues such as R93 in Cry1Ac (46) and R99 in Cry1Aa (41), most alterations in α2 (46), α3 (23, 26, 41, 46), α6 (4), and α7 (1) result in relatively minor effects on toxin function, whereas many of the single-site alterations introduced in α4 (2, 26, 30, 38) and α5 (32, 46) result in greatly reduced activity. Also consistent with an important role of α4 and α5, synthetic peptides corresponding to these helices (10, 17, 19) or to the α4-loop-α5 segment (20) of Cry1Ac or Cry3Aa have been shown to self-assemble and form ion channels in artificial lipid bilayer membranes. In contrast, synthetic peptides corresponding to α2, α3, α6, and α7 were found to bind to the surface of the membrane (18).

In a previous study, mutations of α4-charged residues in Cry1Aa were shown to considerably reduce toxicity to *Plutella xylostella* and the conductance of the pores formed in receptor-free planar lipid bilayers (30). In addition, chemical modification of an engineered cysteine residue, D136C, has provided strong evidence that α4 lines the lumen of the pore (30). More recently, the α4 residue N135 of Cry1Ab and Cry1Ac was shown to play a crucial role in toxin oligomerization and pore formation (39). To further investigate the functional role of α4, the pore-forming properties of mutants in which each charged residue (R127, E128, E129, R131, and D136) in α4 was replaced individually with a neutral or an oppositely charged amino acid were analyzed in brush border membrane vesicles isolated from *Manduca sexta* by using an osmotic swelling permeability assay (6). Almost all of these mutations, as well as the

TABLE 1. Toxicity of Cry1Aa α4 mutants toward *M. sexta* larvae

Toxin	% Mortality[a] at:		
	50 ng/ml	2 μg/ml	50 μg/ml
Cry1Aa	45 ± 1	—[b]	—
R127E	6 ± 1	89 ± 2	—
R127N	22 ± 1	97 ± 1	—
E128C	24 ± 3	92 ± 2	—
E129C	—	7 ± 2	14 ± 2
E129K	—	7 ± 2	8 ± 1
R131D	—	8 ± 1	23 ± 2
R131E	7 ± 2	92 ± 1	—
R131H	—	6 ± 2	7 ± 2
R131Q	7 ± 1	33 ± 1	95 ± 2
D136C	—	7 ± 1	9 ± 1
D136N	—	6 ± 2	17 ± 1
D136Y	—	5 ± 2	8 ± 2
T142D	—	5 ± 2	23 ± 1
T143D	–	10 ± 1	21 ± 1

[a] Values are means ± SEM of five independent experiments.
[b] —, not tested.

replacement of neutral residues (T142 and T143) with aspartic acid, resulted in substantial reductions in the toxicity and pore-forming ability of the toxins.

MATERIALS AND METHODS

Mutagenesis. The mutations analyzed in the present study are listed in Table 1. They were introduced in α4 of Cry1Aa by in vitro site-directed mutagenesis using the double oligonucleotide method (14) (Transformer kit; Clontech Laboratories, Palo Alto, Calif.) and the double-stranded expression plasmid pMP39 (29). All mutants were sequenced using an Applied Biosystems (Foster City, Calif.) model 370A automated fluorescent sequencer.

Toxin production and purification. All toxins were produced in *Escherichia coli* grown at 30°C in double-strength YT broth containing 100 μg of ampicillin/ml (29). The insoluble protoxin-containing inclusions were harvested and activated with 1% (wt/vol) trypsin as described previously (29). Activated toxins were purified by fast protein liquid chromatography using a Mono Q ion exchange column (Pharmacia Biotech, Montreal, Canada) as described elsewhere (29). Toxin purity and integrity were verified by sodium dodecyl sulfate-polyacrylamide gel electrophoresis (27), and protein concentrations were determined by the method of Bradford (5) with bovine serum albumin as a standard.

Bioassays. Fertilized eggs of *M. sexta* were purchased from the Carolina Biological Supply Company (Burlington, N.C.). Toxicity assays were performed on artificial diet (8) as described previously (41) using neonate larvae and trypsin-activated toxins. Mortality was recorded after 7 days. All mutant toxins were tested at 2 μg/ml, and, depending on the percent mortality observed at this concentration, the tests were repeated at either 50 ng/ml or 50 μg/ml. Thirty larvae were used for each toxin concentration tested, and the bioassays were replicated five times.

Preparation of brush border membrane vesicles. *M. sexta* larvae were raised to the fifth instar on the artificial diet supplied with the insects. Whole midguts were isolated, cleared of their contents and attached Malpighian tubules, and stored at −80°C until use. Brush border membrane vesicles were prepared from thawed midguts as described previously (41) using a magnesium precipitation and differential centrifugation method (45).

Light-scattering assay. Brush border membrane permeability was analyzed with a light-scattering assay as described by Carroll and Ellar (6). Osmotic volume changes were monitored by measuring the 90° scattered light intensity at 23°C in a Spex CMIII spectrofluorometer (Jobin Yvon Horiba, Edison, N.J.) with both monochromators set at 450 nm. To test whether the mutations altered the properties of the pores, membrane permeability was measured in the presence of 150 mM KCl, the chloride salt of the relatively large cation *N*-methyl-D-glucamine, the potassium salt of the relatively large anion gluconate, or 300 mM disaccharide sucrose or trisaccharide raffinose. A mutation affecting mainly the number of pores formed would alter membrane permeability to all solutes, relative to that observed with Cry1Aa, to a similar extent. On the other hand, an alteration in pore size is expected to mainly affect membrane permeability to the larger solutes. Finally, a change in ionic selectivity of the pores would result in a stronger effect on the permeability to *N*-methyl-D-glucamine or to gluconate. To evaluate the ability of the toxins to permeabilize the membrane to these various solutes, vesicles were preincubated for 60 min with the selected concentration of toxin before the light-scattering assays were performed as described previously (9, 41). In kinetic experiments designed to estimate the rate at which the toxins increase membrane permeability, vesicles were exposed to the toxin at the onset of the light-scattering experiments as described previously (9, 41).

Data analysis. Percent volume recovery was calculated as $100(1 - I_t)$, where I_t is the relative scattered light intensity measured at time t. For kinetic experiments, percent volume recovery was calculated for each data point and values obtained for control vesicles, assayed without toxin, were subtracted from the experimental values measured in the presence of toxin. The ascending portion of each resulting trace was best fitted with a Boltzmann sigmoid using the Origin version 6.1 program (OriginLab Corp., Northampton, Mass.). The delay preceding vesicle swelling, arbitrarily defined as the time required to reach a percent volume recovery of 5%, was derived directly from these fitted curves. The maximal rate of osmotic swelling was obtained for each trace as the peak value of the first derivative of the sigmoidal fit. Data are reported as means ± standard errors of the means (SEM) of at least three experiments performed with different vesicle preparations. Experimental values for each individual experiment consisted of the average of five replicates obtained using the same vesicle preparation. Statistical comparisons were made with the two-tailed unpaired t test using the Instat version 1.13 program (Graphpad Software, San Diego, Calif.).

RESULTS

Toxicity. Cry1Aa has five charged amino acids in α4, two positively charged ones (R127 and R131) and three negatively charged ones (E128, E129, and D136). The respective position of these amino acids within α4 is shown in Fig. 1. These charged residues are all located on the same side, covering a little more than half of the circumference of the helix, which comprises 10 polar residues out of a total of 17. The other side of the helix has nine residues, including a single polar amino acid (Q133). Most mutants were considerably less toxic to *M. sexta* larvae than Cry1Aa (Table 1). At 2 μg of toxin/ml, only five mutants, R127E, R127N, E128C, R131E, and R131Q, were lethal to more than 10% of the larvae. At 50 ng of toxin/ml, mortality levels observed for R127N and E128C were about twofold lower than those observed for wild-type Cry1Aa, while R127E, R131E, and R131Q caused approximately six- to sevenfold less mortality than Cry1Aa. The least toxic mutants were E129K, R131H, D136C, and D136Y, for which mortalities below 10% were observed at 50 μg of toxin/ml.

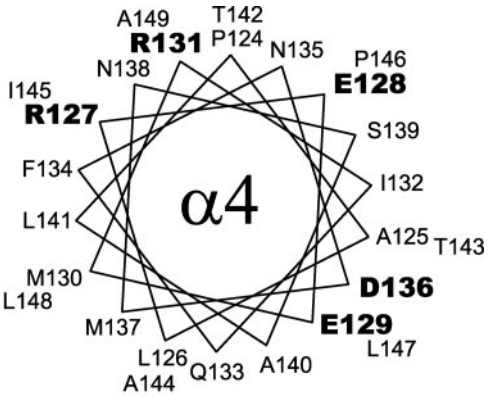

FIG. 1. Amino acid sequence and helical wheel representation of α4 from Cry1Aa. Charged residues, in which mutations were introduced, are identified by boldface.

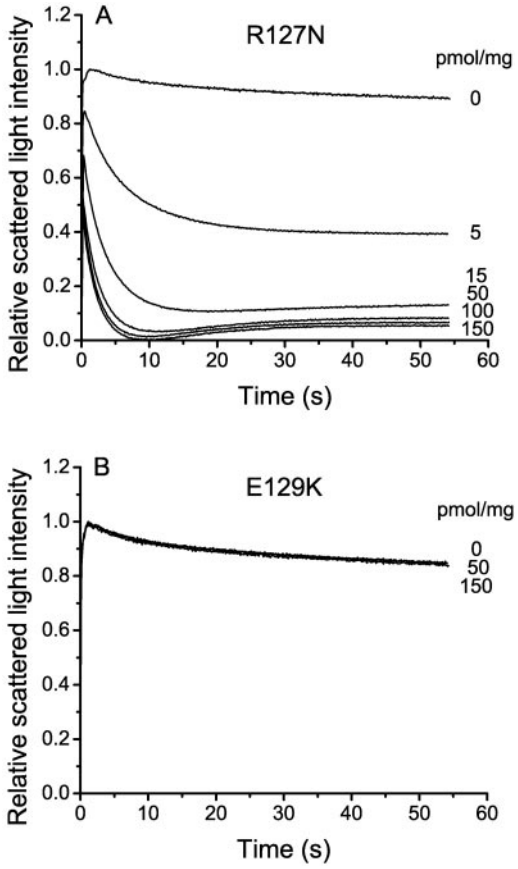

FIG. 2. Effect of α4 mutants on the osmotic swelling of *M. sexta* brush border membrane vesicles. Midgut membrane vesicles isolated from fifth-instar *M. sexta* larvae and equilibrated overnight in 10 mM HEPES-KOH (pH 7.5) were preincubated for 60 min with the indicated concentrations (in picomoles of toxin/milligram of membrane protein) of either R127N (A) or E129K (B). Vesicles were rapidly mixed with an equal volume of 150 mM KCl and 10 mM HEPES-KOH (pH 7.5) directly in a cuvette using a stopped-flow apparatus. Each trace corresponds to the average of five experiments.

Pore-forming ability. The pore-forming properties of these mutants were analyzed with an osmotic swelling assay (6). In this assay, permeability to a given solute is evaluated by measuring scattered light intensity following rapid mixing of the vesicles with a hypertonic solution of the solute. The ensuing osmotic shrinking of the vesicles is detected by a rapid rise in scattered light intensity (Fig. 2). As the solute diffuses into the vesicles, these swell at a rate and to an extent that depend on the permeability of the membrane to the solute. Membrane permeability increases rapidly with increasing concentration of an active toxin, as illustrated by R127N, the mutant with the highest toxicity, and among those with the strongest pore-forming ability (Fig. 2A). In contrast, with an inactive mutant, such as E129K, the vesicle-swelling rate was identical to that observed with control vesicles and was independent of toxin concentration (Fig. 2B).

The highly alkaline conditions, characteristic of the lepidopteran midgut lumen, are thought to play an important role in *B. thuringiensis* toxin function (36). The pore-forming ability of some toxins, including Cry1C (40) and several Cry1Aa α3 mutants (41), has indeed been shown to be strongly modulated by pH. Experiments were therefore carried out at both pH 7.5 and 10.5. Altering charged residues within α4 caused drastic reductions in the pore-forming ability of most mutant toxins (Fig. 3), with the exception of R127E, R127N (Fig. 3A and B), and R131H (Fig. 3G and H), as well as R131D at pH 7.5 (Fig. 3G). The most dramatic losses of activity were observed for E129C, E129K (Fig. 3E and F), and D136Y (Fig. 3I and J). In addition, introducing a negatively charged aspartic acid in T142D and T143D, near the C-terminal end of the helix, which is normally devoid of charged residues, resulted in a complete loss of activity (Fig. 3K and L). Increasing pH from 7.5 to 10.5 had little effect on the inactive mutants or on Cry1Aa, R127E, or R127N (Fig. 3A and B), but considerably reduced activity was observed at the higher pH for all mutants with alterations at position 131, except for R131H (Fig. 3G and H). In contrast, vesicle permeability to KCl was higher at pH 10.5 than at pH 7.5 in the presence of E128C (Fig. 3C and D) and D136C (Fig. 3I and J).

Kinetics of pore formation. All mutants that retained a detectable pore-forming ability according to the preincubation assay results (Fig. 3) were further tested to evaluate the rate at which they increased membrane permeability. This increase was measured by monitoring percent volume recovery as a function of time after exposing the vesicles simultaneously to the toxin and to a KCl gradient (Fig. 4). In the presence of an active toxin, the resulting traces are characterized by a sigmoidal increase in percent volume recovery. Two kinetic parameters were derived from Boltzmann sigmoidal curves fitted to each experimental trace: the delay preceding the time at which percent volume recovery reached 5% and the maximal rate of increase in percent volume recovery, corresponding to the slope of the curves at their inflection point and determined as the peak value of the first derivative of the fitted curves (Table 2). In agreement with their strong pore-forming ability following a 1-h preincubation with the vesicles (Fig. 3), R127E and R127N were the most active among the mutants tested, displaying the shortest delays and highest vesicle-swelling rates. Nevertheless, R127E had significantly less activity than Cry1Aa and R127N in the kinetic assay, especially at pH 10.5 (Fig. 4), which correlated well with its lower toxicity (Table 1). The other mutants were all significantly less active than Cry1Aa, with more than threefold longer delays and more than fourfold lower rates of vesicle swelling (Table 2). Except for E128C, D136C, D136N, and Cry1Aa, all toxins permeabilized the membrane after a significantly longer delay ($P < 0.01$) and at a significantly lower rate ($P < 0.01$) at pH 10.5 than at pH 7.5.

Pore properties. The properties of the pores formed by the various active mutants were further investigated by measuring their permeability to the large uncharged solutes, sucrose and raffinose (Fig. 5), and to the large ions, *N*-methyl-D-glucamine and gluconate (Fig. 6). As expected from its smaller size, sucrose diffused faster than raffinose across the pores formed by the toxins. In agreement with their higher permeability to KCl (Fig. 3), the pores formed by R127E, R127N, and R131H displayed a higher permeability to sucrose (Fig. 5A and B) and raffinose (Fig. 5C and D) than those formed by all of the other mutants. At variance with the KCl permeability data (Fig. 3), however, the pores formed by R131D were significantly less permeable than those formed by Cry1Aa to both sugars. Those

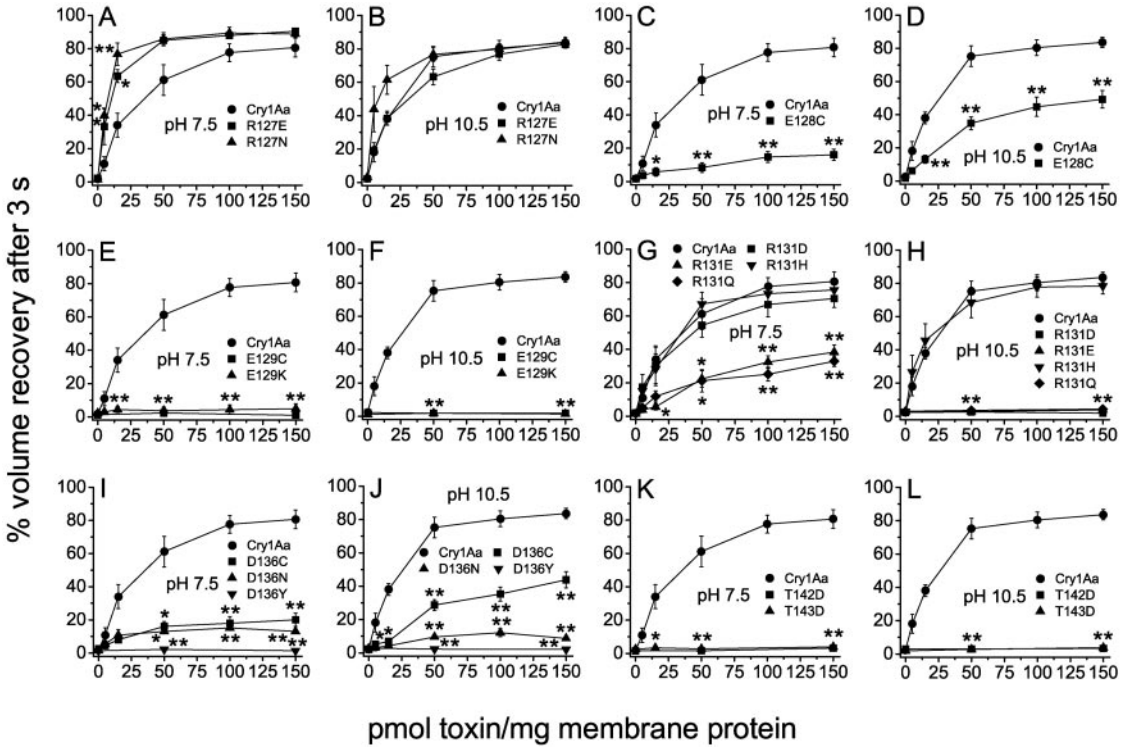

FIG. 3. Pore-forming ability of α4 mutants. Brush border membrane vesicles equilibrated overnight in 10 mM either HEPES-KOH (pH 7.5) (A, C, E, G, I, and K) or CAPS (3-cyclohexylamino-1-propanesulfonic acid)-KOH (pH 10.5) (B, D, F, H, J, and L) were preincubated for 60 min with the indicated concentrations of either Cry1Aa or one of its mutants with alterations at amino acid positions 127 (A and B), 128 (C and D), 129 (E and F), 131 (G and H), 136 (I and J), or 142 and 143 (K and L). Their permeability to KCl was monitored following rapid mixing with 150 mM KCl and 10 mM either HEPES-KOH (pH 7.5) (A, C, E, G, I, and K) or CAPS-KOH (pH 10.5) (B, D, F, H, J, and L). Percent volume recovery was calculated for the 3-s time point from traces like those shown in Fig. 2. Data are means ± SEM of at least three independent experiments. Asterisks indicate statistically significant differences with the corresponding values obtained for wild-type Cry1Aa (*, $P < 0.05$; **, $P < 0.01$).

formed by R131H were also significantly less permeable to sucrose at pH 7.5 and to raffinose at pH 10.5. The pores formed by Cry1Aa and Cry1Ac have previously been shown to be more permeable to sucrose at pH 10.5 than at pH 7.5, suggesting a slightly larger pore diameter at the higher pH (7, 9, 40, 41). Although higher permeabilities to sucrose were observed at pH 10.5, with most mutants capable of forming pores at both pH values, none of these increases was statistically significant ($P > 0.05$).

In agreement with the fact that the pores formed by *B. thuringiensis* toxins are generally cation selective, higher osmotic swelling rates were observed in the presence of *N*-methyl-D-glucamine hydrochloride (Fig. 6A) than with potassium gluconate (Fig. 6B and C) (25). Because *N*-methyl-D-glucamine is not ionized at pH 10.5, experiments with this compound were only conducted at pH 7.5. As was observed with the other solutes, membrane permeability to both *N*-methyl-D-glucamine hydrochloride and potassium gluconate in the presence of R127E, R127N, or R131H was similar to that observed with Cry1Aa, although the pores formed by R127N were significantly more permeable to *N*-methyl-D-glucamine ($P < 0.05$) than those formed by Cry1Aa (Fig. 6A) and those formed by R131H were significantly less permeable to potassium gluconate at pH 7.5 (Fig. 6B). The pores formed by all other mutants were significantly less permeable to both solutes than those formed by Cry1Aa.

DISCUSSION

The results of the present study confirm and extend a previous demonstration that most mutations altering charged residues of α4 result in strong reductions in the toxicity and pore-forming properties of Cry1Aa (30). Although the larvae of *M. sexta* were more sensitive to Cry1Aa than those of *P. xylostella* (studied previously), E129K, R131D, R131Q, D136C, and D136N were poorly toxic, and R127N was only slightly less toxic than the wild-type toxin, for both species. However, although R127E and R127N displayed a similar toxicity to *P. xylostella*, the former mutant was less toxic than the latter to *M. sexta*. With the exception of E128C and R131E, the additional mutants with charge alterations or additions in α4 residues included in the present study, E129C, R131H, D136Y, T142D, and T143D, were all essentially nontoxic to *M. sexta* larvae. Charge alterations in α4 residues that reduce the toxicity of other *B. thuringiensis* toxins include R131L and Q133R from Cry1Ac (26), R158A from Cry4Ba (38), and K123A, R136A, R136D, R136K, R136Q, and E141A from Cry11A (2). However, other mutations altering α4 charged residues, including R131C and R131S, had no significant effect on the toxicity of Cry1Ac (26), nor did R143A and E159A affect that of Cry4Ba (38).

The mutants E129K, D136C, and D136N have been previously shown to be considerably less active than Cry1Aa in

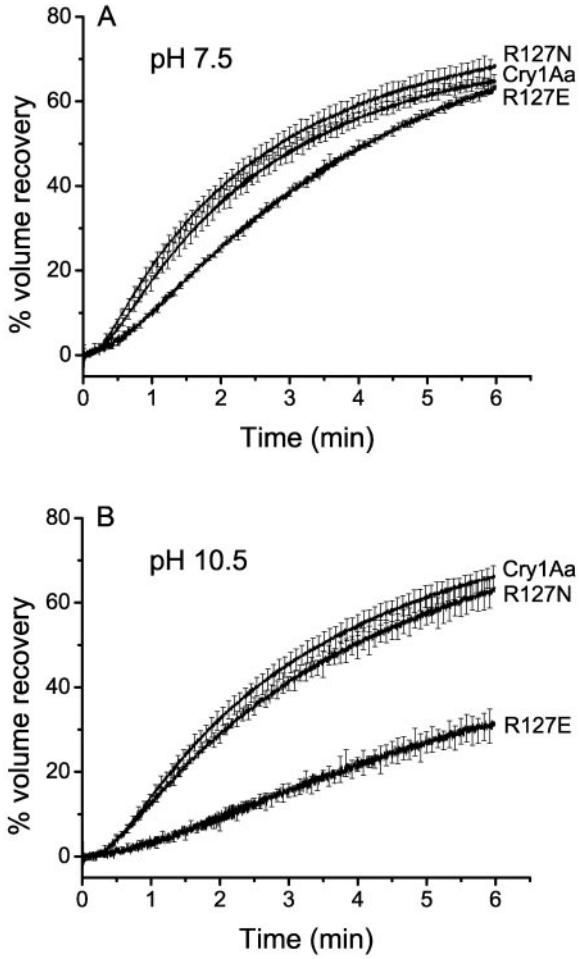

FIG. 4. Kinetics of pore formation. Brush border membrane vesicles equilibrated overnight in 10 mM either HEPES-KOH (pH 7.5) (A) or CAPS (3-cyclohexylamino-1-propanesulfonic acid)-KOH (pH 10.5) (B) were mixed with an equal volume of 150 mM KCl and 10 mM either HEPES-KOH (pH 7.5) (A) or CAPS-KOH (pH 10.5) (B) and 150 pmol of toxin/mg of membrane protein of Cry1Aa, R127E, or R127N, without preincubation. Percent volume recovery was calculated for each experimental point, and control values were subtracted from those obtained in the presence of toxin. For clarity, error bars (SEM) are shown only for every 50th data point.

planar lipid bilayer experiments (30). While lipid bilayer studies allow a detailed analysis of the properties of the pores at the single-channel level, osmotic swelling experiments, such as those presented herein, are better suited for characterizing overall toxin pore-forming ability and rates of pore formation. In addition, these experiments were carried out using vesicles prepared from the midgut brush border membrane, which constitutes the natural target of these toxins and therefore possesses the toxin receptors of the insect species from which it was isolated. Our choice of *M. sexta* for the present study was motivated by the fact that large quantities of tightly sealed and osmotically active vesicles can be prepared with much greater ease from this species than from small insects such as *P. xylostella*. This choice also has the advantage of allowing a direct comparison with previous studies using the same experimental system and in which mutations were introduced elsewhere in Cry1Aa (9, 41).

For most of the mutants, losses in toxicity correlated well with significant reductions in pore-forming ability and reduced rates of pore formation. The only exceptions were E128C and R131E, which retained a relatively strong toxicity despite a significantly reduced pore-forming ability, and R131H and R131D, which were poorly toxic but displayed a pore-forming ability that was comparable to that of Cry1Aa, although R131D completely lost its capacity to form pores at pH 10.5. Examples of toxins with poor toxicity that readily form pores in brush border membrane vesicles have been reported previously (9, 40, 41). Although such differences between in vivo and in vitro toxin activities require further study, they are probably attributable to reduced toxin stability in the presence of midgut proteases and emulsifying agents. E128C and R131E, however, appear to be stable enough to kill insect larvae even though they form pores significantly less efficiently than Cry1Aa during the much smaller time frame of the in vitro experiments.

Interestingly, R131D was significantly more active than R131E at pH 7.5 in the osmotic swelling assay, despite the fact that these two toxins differ by a single methylene group. This result indicates that the deleterious effect of inverting the positive charge at this position is amplified by increasing the length of the side chain of the negatively charged amino acid. The effect of this charge alteration was greatly amplified at pH 10.5, at which both toxins were completely inactive. This suggests an unfavorable interaction of the negative charge with one or more amino acid residues that are titrated between pH 7.5 and 10.5, such as lysine and tyrosine. The involvement of a lysine residue appears unlikely because the activated Cry1Aa has only two such residues, both in domain III. On the other hand, 11 tyrosine residues are present in domain I, scattered among all helices except α2 and α4. At variance with these in vitro data, however, R131E was more toxic to the larvae than R131D, even though both toxins were considerably less toxic than wild-type Cry1Aa. Additional factors, possibly including ionic strength and the presence of a strong membrane potential, thus appear to modulate toxin activity as was suggested previously (40).

Toxin-induced membrane permeability depends not only on the efficiency with which pores are formed within the mem-

TABLE 2. Kinetics of pore formation by Cry1Aa α4 mutants in *M. sexta* midgut brush border membrane vesicles

Toxin	Delay[a] (min)		Swelling rate[b] (% vol recovery/min)	
	pH 7.5	pH 10.5	pH 7.5	pH 10.5
Cry1Aa	0.45 ± 0.03	0.57 ± 0.04	26.7 ± 3.3	23.5 ± 1.8
R127E	0.64 ± 0.02**[c]	1.33 ± 0.13**	15.4 ± 0.3	6.6 ± 0.7**
R127N	0.38 ± 0.03	0.58 ± 0.02	30.1 ± 1.9	19.3 ± 0.9
E128C	3.06 ± 0.40**	4.01 ± 0.22**	2.7 ± 0.3**	2.0 ± 0.2**
R131D	1.35 ± 0.15**	NA[d]	6.2 ± 0.5**	NA
R131E	1.42 ± 0.20**	NA	6.2 ± 0.8**	NA
R131H	1.61 ± 0.24**	>6.00	6.7 ± 0.6**	0.4 ± 0.3**
R131Q	2.24 ± 0.32**	NA	3.5 ± 0.6**	NA
D136C	2.89 ± 0.56**	1.84 ± 0.22**	4.1 ± 0.4**	5.4 ± 0.9**
D136N	2.03 ± 0.26**	3.17 ± 0.42**	4.5 ± 0.1**	3.0 ± 0.8**

[a] Time required for volume recovery to reach 5%.
[b] Slope at the inflection point of the Boltzmann sigmoidal curves fitted to the data points.
[c] **, Significantly different from the corresponding value obtained for Cry1Aa ($P < 0.01$).
[d] NA, not active at pH 10.5.

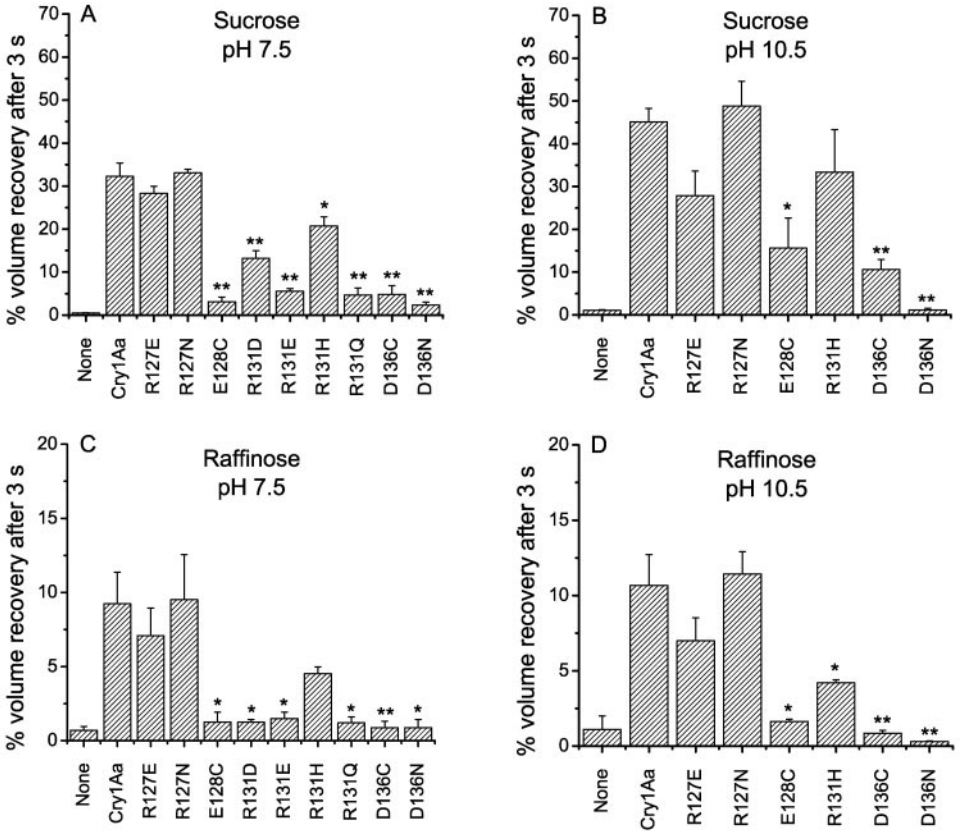

FIG. 5. Effect of α4 mutants on vesicle permeability to oligosaccharides. Vesicles equilibrated in 10 mM either HEPES-KOH (pH 7.5) (A and C) or CAPS (3-cyclohexylamino-1-propanesulfonic acid)-KOH (pH 10.5) (B and D) were preincubated for 60 min with 150 pmol of toxin/mg of membrane protein. Their permeability to sucrose (A and B) and raffinose (C and D) was monitored following rapid mixing with 300 mM either sucrose or raffinose and 10 mM either HEPES-KOH (pH 7.5) (A and C) or CAPS-KOH (pH 10.5) (B and D) as described in the legends of Fig. 2 and 3. Asterisks indicate statistically significant differences with Cry1Aa (*, $P < 0.05$; **, $P < 0.01$).

brane but also on the biophysical properties of the pores, including their diameter and ion selectivity. To evaluate the possible effect of the mutations on these parameters, all mutants that retained a detectable pore-forming ability with KCl were tested for their capacity to permeabilize the membrane to relatively large solutes which included both neutral and charged species. For most mutants, permeability to each of these solutes was affected to an extent which closely paralleled that observed with KCl. This clearly indicates that the major effect of most mutations analyzed was a substantial reduction in the ability of the toxins to form functional pores. Possible exceptions include R131D which, even though it was not functional at pH 10.5, displayed a permeability to KCl at pH 7.5 which was similar to that observed with Cry1Aa but was significantly lower to each of the larger solutes. In the presence of R131H, permeability to KCl was similar to that observed with Cry1Aa at both pH values, but permeability to sucrose and potassium gluconate at pH 7.5 and to raffinose at pH 10.5 was significantly lower. These results suggest that R131D and R131H could form pores with a somewhat smaller diameter than those formed by Cry1Aa.

Changes in pH strongly affect the pore-forming ability of certain *B. thuringiensis* toxins, such as Cry1C, while having only minor effects on the activity of others, such as Cry1Ac (40). In the present study, Cry1Aa and most of its mutants were not significantly affected by this factor in the preincubation assays, even though almost all mutants were less active at the higher pH in the kinetic assay. Increasing pH from 7.5 to 10.5, however, completely abolished the ability of R131D, R131E, and R131Q to form pores. A few cases of Cry1Aa mutants that formed pores less efficiently at the higher pH have been reported earlier (41). In contrast, E128C and D136C were significantly more active at pH 10.5 than at pH 7.5. The thiol group of cysteine has a pK_a of 8.3 (35). This increase in toxin activity therefore coincides with the restoration of the negative charge normally present at these positions in the wild-type toxin. Such pH-dependent increases in toxin activity have not been observed in other cases where a negatively charged amino acid was replaced by a cysteine, including the α3 mutants E101C and E118C (41) and the α4 mutant E129C. These findings suggest that a negative charge on residues 128 and 136 contributes significantly to the activity of Cry1Aa, even though the sole presence of a negative charge at these positions was clearly insufficient to restore the toxin's full activity. These results are also consistent with earlier demonstrations that the thiol group of D136C is accessible to chemical modification within the lumen of the pore and that adding a negative charge to this residue in situ results in a substantially increased conductance and probability the pores will be open (30). The fact that pH affects the activity of E128C and D136C in a similar

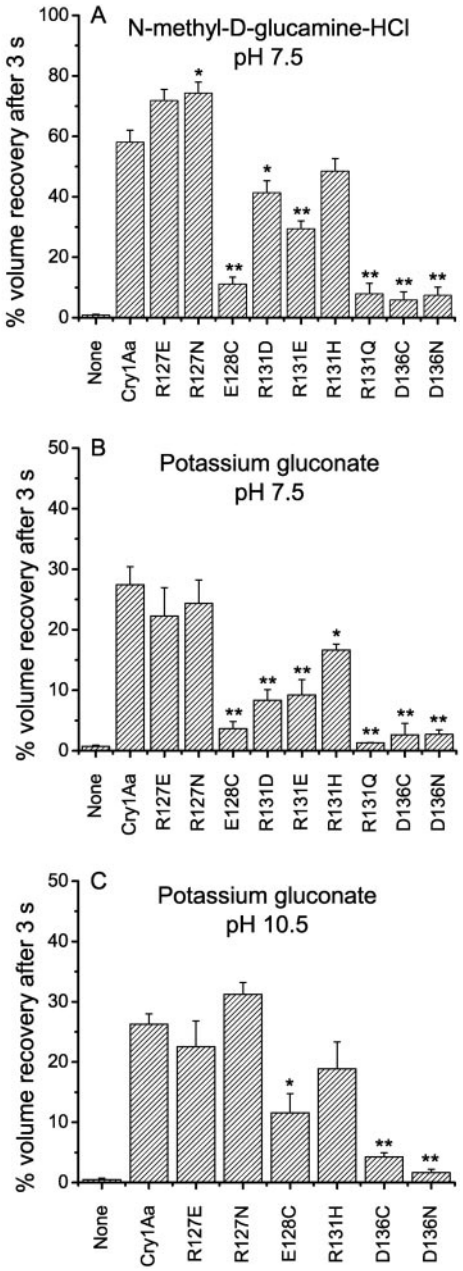

FIG. 6. Effect of α4 mutants on vesicle permeability to *N*-methyl-D-glucamine hydrochloride and potassium gluconate. Vesicles equilibrated in 10 mM either HEPES-KOH (pH 7.5) (A and B) or CAPS (3-cyclohexylamino-1-propanesulfonic acid)-KOH (pH 10.5) (C) were preincubated for 60 min with 150 pmol of toxin/mg of membrane protein. Their permeability to *N*-methyl-D-glucamine hydrochloride (A) and potassium gluconate (B and C) was monitored following rapid mixing with 150 mM either *N*-methyl-D-glucamine hydrochloride or potassium gluconate and 10 mM either HEPES-KOH (pH 7.5) (A and B) or CAPS-KOH (pH 10.5) (C) as described in the legends of Fig. 2 and 3. Asterisks indicate statistically significant differences with Cry1Aa (*, $P < 0.05$; **, $P < 0.01$).

manner suggests that the negative charge on E128 plays an important role in the formation of functional pores, possibly by ensuring that a high proportion of the channels are in their open state. Alternatively, this residue could be involved in the oligomerization of the toxin, as suggested by its close proximity with N135, which has been clearly shown to be essential for this aspect of pore formation (39).

In conclusion, our results, along with those of previous studies (2, 26, 30, 38, 39), provide further evidence that the functional properties of *B. thuringiensis* toxins are strongly influenced by mutations altering α4 residues. They also indicate that this helix is critically involved not only in the architecture of the pores (30) but also in the mechanism by which toxin molecules insert into the membrane to form a functional pore.

ACKNOWLEDGMENTS

This work was supported by grants from the Natural Sciences and Engineering Research Council of Canada to R.L. and J.L.S. F.C. was supported by a scholarship for doctoral studies from the Ministère de l'Éducation et de la Recherche of France.

REFERENCES

1. **Alcantara, E. P., O. Alzate, M. K. Lee, A. Curtiss, and D. H. Dean.** 2001. Role of α-helix seven of *Bacillus thuringiensis* Cry1Ab δ-endotoxin in membrane insertion, structural stability, and ion channel formation. Biochemistry **40:**2540–2547.
2. **Angsuthanasombat, C., S. Keeratichamreon, S. Leetacheewa, G. Katzenmeier, and S. Panyim.** 2001. Directed mutagenesis of the *Bacillus thuringiensis* Cry11A toxin reveals a crucial role in larval activity of arginine-136 in helix 4. J. Biochem. Mol. Biol. **34:**402–407.
3. **Aronson, A. I., and Y. Shai.** 2001. Why *Bacillus thuringiensis* insecticidal toxins are so effective: unique features of their mode of action. FEMS Microbiol. Lett. **195:**1–8.
4. **Aronson, A. I., D. Wu, and C. Zhang.** 1995. Mutagenesis of specificity and toxicity regions of a *Bacillus thuringiensis* protoxin gene. J. Bacteriol. **177:** 4059–4065.
5. **Bradford, M. M.** 1976. A rapid and sensitive method for the quantitation of microgram quantities of protein utilizing the principle of protein-dye binding. Anal. Biochem. **72:**248–254.
6. **Carroll, J., and D. J. Ellar.** 1993. An analysis of *Bacillus thuringiensis* δ-endotoxin action on insect-midgut-membrane permeability using a light-scattering assay. Eur. J. Biochem. **214:**771–778.
7. **Carroll, J., and D. J. Ellar.** 1997. Analysis of the large aqueous pores produced by a *Bacillus thuringiensis* protein insecticide in *Manduca sexta* midgut-brush-border-membrane vesicles. Eur. J. Biochem. **245:**797–804.
8. **Couilloud, R., and M. Giret.** 1980. Multiplication d'*H. armigera* Hbn (Lep. Noctuidae): améliorations possibles grâce à l'adaptation d'une technique d'élevage en groupe des chenilles. Coton Fibres Trop. **35:**217–224.
9. **Coux, F., V. Vachon, C. Rang, K. Moozar, L. Masson, M. Royer, M. Bes, S. Rivest, R. Brousseau, J.-L. Schwartz, R. Laprade, and R. Frutos.** 2001. Role of interdomain salt bridges in the pore-forming ability of the *Bacillus thuringiensis* toxins Cry1Aa and Cry1Ac. J. Biol. Chem. **276:**35546–35551.
10. **Cummings, C. E., G. Armstrong, T. C. Hodgman, and D. J. Ellar.** 1994. Structural and functional studies of a synthetic peptide mimicking a proposed membrane inserting region of a *Bacillus thuringiensis* δ-endotoxin. Mol. Membr. Biol. **11:**87–92.
11. **de Maagd, R. A., P. L. Bakker, L. Masson, M. J. Adang, S. Sangadala, W. Stiekema, and D. Bosch.** 1999. Domain III of the *Bacillus thuringiensis* delta-endotoxin Cry1Ac is involved in binding to *Manduca sexta* brush border membranes and to its purified aminopeptidase N. Mol. Microbiol. **31:**463–471.
12. **de Maagd, R. A., P. Bakker, N. Staykov, S. Dukiandjiev, W. Stiekema, and D. Bosch.** 1999. Identification of *Bacillus thuringiensis* delta-endotoxin Cry1C domain III amino acid residues involved in insect specificity. Appl. Environ. Microbiol. **65:**4369–4374.
13. **de Maagd, R. A., D. Bosch, and W. Stiekema.** 1999. *Bacillus thuringiensis* toxin-mediated insect resistance in plants. Trends Plant Sci. **4:**9–13.
14. **Deng, W. P., and J. A. Nickoloff.** 1992. Site-directed mutagenesis of virtually any plasmid by eliminating a unique site. Anal. Biochem. **200:**81–88.
15. **Frutos, R., C. Rang, and M. Royer.** 1999. Managing insect resistance to plants producing *Bacillus thuringiensis* toxins. Crit. Rev. Biotechnol. **19:**227–276.
16. **Galitsky, N., V. Cody, A. Wojtczak, D. Ghosh, J. R. Luft, W. Pangborn, and L. English.** 2001. Structure of the insecticidal bacterial δ-endotoxin Cry3Bb1 of *Bacillus thuringiensis*. Acta Crystallogr. Sect. D Biol. Crystallogr. **57:**1101–1109.
17. **Gazit, E., D. Bach, I. D. Kerr, M. S. P. Sansom, N. Chejanovsky, and Y. Shai.** 1994. The α-5 segment of *Bacillus thuringiensis* δ-endotoxin: in vitro activity, ion channel formation and molecular modelling. Biochem. J. **304:**895–902.
18. **Gazit, E., P. La Rocca, M. S. P. Sansom, and Y. Shai.** 1998. The structure and organization within the membrane of the helices composing the pore-

forming domain of *Bacillus thuringiensis* δ-endotoxin are consistent with an "umbrella-like " structure of the pore. Proc. Natl. Acad. Sci. USA **95:**12289–12294.
19. **Gazit, E., and Y. Shai.** 1993. Structural and functional characterization of the α5 segment of *Bacillus thuringiensis* δ-endotoxin. Biochemistry **32:**3429–3436.
20. **Gerber, D., and Y. Shai.** 2000. Insertion and organization within membranes of the δ-endotoxin pore-forming domain, helix 4-loop-helix 5, and inhibition of its activity by a mutant helix 4 peptide. J. Biol. Chem. **275:**23602–23607.
21. **Grochulski, P., L. Masson, S. Borisova, M. Pusztai-Carey, J.-L. Schwartz, R. Brousseau, and M. Cygler.** *Bacillus thuringiensis* CryIA(a) insecticidal toxin: crystal structure and channel formation. J. Mol. Biol. **254:**447–464.
22. **Höfte, H., and H. R. Whiteley.** 1989. Insecticidal crystal proteins of *Bacillus thuringiensis*. Microbiol. Rev. **53:**242–255.
23. **Hussain, S.-R. A., A. I. Aronson, and D. H. Dean.** 1996. Substitution of residues on the proximal side of Cry1A *Bacillus thuringiensis* δ-endotoxins affects irreversible binding to *Manduca sexta* midgut membrane. Biochem. Biophys. Res. Commun. **226:**8–14.
24. **Jenkins, J. L., M. K. Lee, A. P. Valaitis, A. Curtiss, and D. H. Dean.** 2000. Bivalent sequential binding model of a *Bacillus thuringiensis* toxin to gypsy moth aminopeptidase N receptor. J. Biol. Chem. **275:**14423–14431.
25. **Kirouac, M., V. Vachon, J.-F. Noël, F. Girard, J.-L. Schwartz, and R. Laprade.** 2002. Amino acid and divalent ion permeability of the pores formed by the *Bacillus thuringiensis* toxins Cry1Aa and Cry1Ac in insect midgut brush border membrane vesicles. Biochim. Biophys. Acta **1561:**171–179.
26. **Kumar, A. S. M., and A. I. Aronson.** 1999. Analysis of mutations in the pore-forming region essential for insecticidal activity of a *Bacillus thuringiensis* δ-endotoxin. J. Bacteriol. **181:**6103–6107.
27. **Laemmli, U. K.** 1970. Cleavage of structural proteins during the assembly of the head of bacteriophage T4. Nature **227:**680–685.
28. **Li, J., J. Carroll, and D. J. Ellar.** 1991. Crystal structure of insecticidal δ-endotoxin from *Bacillus thuringiensis* at 2.5 Å resolution. Nature **353:**815–821.
29. **Masson, L., G. Préfontaine, L. Péloquin, P. C. K. Lau, and R. Brousseau.** 1989. Comparative analysis of the individual protoxin components in P1 crystals of *Bacillus thuringiensis subsp. kurstaki* isolates NRD-12 and HD-1. Biochem. J. **269:**507–512.
30. **Masson, L., B. E. Tabashnik, Y.-B. Liu, R. Brousseau, and J.-L. Schwartz.** 1999. Helix 4 of the *Bacillus thuringiensis* Cry1Aa toxin lines the lumen of the ion channel. J. Biol. Chem. **274:**31996–32000.
31. **Morse, R. J., T. Yamamoto, and R. M. Stroud.** 2001. Structure of Cry2Aa suggests an unexpected receptor binding epitope. Structure **9:**409–417.
32. **Nuñez-Valdez, M.-E., J. Sánchez, L. Lina, L. Güereca, and A. Bravo.** 2001. Structural and functional studies of α-helix 5 region from *Bacillus thuringiensis* Cry1Ab δ-endotoxin. Biochim. Biophys. Acta **1546:**122–131.
33. **Rang, C., V. Vachon, F. Coux, C. Carret, W. J. Moar, R. Brousseau, J.-L. Schwartz, R. Laprade, and R. Frutos.** 2001. Exchange of domain I from *Bacillus thuringiensis* Cry1 toxins influences protoxin stability and crystal formation. Curr. Microbiol. **43:**1–6.
34. **Rang, C., V. Vachon, R. A. de Maagd, M. Villalon, J.-L. Schwartz, D. Bosch, R. Frutos, and R. Laprade.** 1999. Interaction between functional domains of *Bacillus thuringiensis* insecticidal crystal proteins. Appl. Environ. Microbiol. **65:**2918–2925.
35. **Rawn, J. D.** 1989. Biochemistry, p. 59. Neil Patterson Publishers, Burlington, N.C.
36. **Schnepf, E., N. Crickmore, J. Van Rie, D. Lereclus, J. Baum, J. Feitelson, D. R. Zeigler, and D. H. Dean.** 1998. *Bacillus thuringiensis* and its pesticidal crystal proteins. Microbiol. Mol. Biol. Rev. **62:**775–806.
37. **Schwartz, J.-L., M. Juteau, P. Grochulski, M. Cygler, G. Préfontaine, R. Brousseau, and L. Masson.** 1997. Restriction of intramolecular movements within the Cry1Aa toxin molecule of *Bacillus thuringiensis* through disulfide bond engineering. FEBS Lett. **410:**397–402.
38. **Sramala, I., S. Leetacheewa, C. Krittanai, G. Katzenmeier, S. Panyim, and C. Angsuthanasombat.** 2001. Charged residue screening in helix 4 of the *Bacillus thuringiensis* Cry4B toxin reveals one critical residue for larvicidal activity. J. Biochem. Mol. Biol. Biophys. **5:**219–225.
39. **Tigue, N. J., J. Jacoby, and D. J. Ellar.** 2001. The α-helix 4 residue, Asn135, is involved in the oligomerization of Cry1Ac1 and Cry1Ab5 *Bacillus thuringiensis* toxins. Appl. Environ. Microbiol. **67:**5715–5720.
40. **Tran, L. B., V. Vachon, J.-L. Schwartz, and R. Laprade.** 2001. Differential effects of pH on the pore-forming properties of *Bacillus thuringiensis* insecticidal crystal toxins. Appl. Environ. Microbiol. **67:**4488–4494.
41. **Vachon, V., G. Préfontaine, F. Coux, C. Rang, L. Marceau, L. Masson, R. Brousseau, R. Frutos, J.-L. Schwartz, and R. Laprade.** 2002. Role of helix 3 in pore formation by the *Bacillus thuringiensis* insecticidal toxin Cry1Aa. Biochemistry **41:**6178–6184.
42. **Van Rie, J.** 2000. *Bacillus thuringiensis* and its use in transgenic insect control technologies. Int. J. Med. Microbiol. **290:**463–469.
43. **Von Tersch, M. A., S. L. Slatin, C. A. Kulesza, and L. H. English.** 1994. Membrane-permeabilizing activities of *Bacillus thuringiensis* coleopteran-active toxin CryIIIB2 and CryIIIB2 domain I peptide. Appl. Environ. Microbiol. **60:**3711–3717.
44. **Walters, F. S., S. L. Slatin, C. A. Kulesza, and L. H. English.** 1993. Ion channel activity of N-terminal fragments from CryIA(c) delta-endotoxin. Biochem. Biophys. Res. Commun. **196:**921–926.
45. **Wolfersberger, M., P. Luethy, A. Maurer, P. Parenti, F. V. Sacchi, B. Giordana, and G. M. Hanozet.** 1987. Preparation and partial characterization of amino acid transporting brush border membrane vesicles from the larval midgut of the cabbage butterfly (*Pieris brassicae*). Comp. Biochem. Physiol. **86A:**301–308.
46. **Wu, D., and A. I. Aronson.** 1992. Localized mutagenesis defines regions of the *Bacillus thuringiensis* δ-endotoxin involved in toxicity and specificity. J. Biol. Chem. **267:**2311–2317.
47. **Wu, S.-J., and D. H. Dean.** 1996. Functional significance of loops in the receptor binding domain of *Bacillus thuringiensis* CryIIIA δ-endotoxin. J. Mol. Biol. **255:**628–640.